

# Half-metallicity of graphene nanoribbons and related systems: a new quantum mechanical El Dorado for nanotechnologies ... or a hype for materials scientists?

Michael S. Deleuze · Matija Huzak · Balázs Hajgató

Received: 23 May 2012 / Accepted: 21 June 2012 / Published online: 24 July 2012  
© Springer-Verlag 2012

**Abstract** In this work we discuss in some computational and analytical details the issue of half-metallicity in zig-zag graphene nanoribbons and nanoislands of finite width, i.e. the coexistence of metallic nature for electrons with one spin orientation and insulating nature for the electrons of opposite spin, which has been recently predicted from so-called first-principle calculations employing Density Functional Theory. It is mathematically demonstrated and computationally verified that, within the framework of non-relativistic and time-independent quantum mechanics, like the size-extensive spin-contamination to which it relates, half-metallicity is nothing else than a methodological artefact, due to a too approximate treatment of electron correlation in the electronic ground state.

**Keywords** Graphene nanoribbons · Edge states · Anti-ferromagnetism · Symmetry breakings · Symmetry restoring · Spin contamination · Electron correlation

## Introduction

Since their first successful experimental fabrication by micromechanical exfoliation of graphite [1], graphenes have been subject of extensive experimental and theoretical research. Long-range  $\pi$ -conjugation in graphene yields

extraordinary thermal, mechanical, and electrical properties. Some of the most significant properties include ballistic electron transport and high current density sustainability [2], quasi-relativistic electron behavior [3, 4], anomalous integer quantum Hall effect at room temperature [5] and fractional quantum Hall effect at low temperatures [6, 7]. The current industrial usage of graphenes is still practically zero, but numerous experimental electronic devices ranging from solar cells and light-emitting devices to touch screens, photodetectors and ultrafast lasers [8, 9] already exist, as well as nanocomposite materials [10].

Unlike the tubular shaped carbon nanotubes, graphene nanoribbons, which are long and narrow strips cut out of a two-dimensional graphene sheet, are known from “first principle” theoretical studies [11–14] employing Density Functional Theory (DFT) [15–17] to present long and reactive zig-zag edges prone to a localization of frontier electronic states, which form a twofold degenerate flat band at the Fermi energy level ( $E_F$ ), within one third of the first Brillouin zone (BZ). The existence of localized electronic edge states has been correspondingly confirmed in monoatomic graphitic step edges using scanning tunnelling microscopy and spectroscopy [18–20]. A most extraordinary property of zig-zag graphene nanoribbons (ZGNRs), which has been theoretically speculated [21] from spin-unrestricted DFT calculations employing the local spin density approximation (LSDA) [22], but never proven, neither experimentally nor by many-body quantum mechanics, is that of half-metallicity, i.e. the coexistence of metallic nature for electrons with one spin orientation and insulating nature for the electrons of opposite spin. This property arises from single-reference spin-unrestricted DFT calculations because of a spontaneous spin-polarization of the electronic ground state. In this depiction, localized electronic states at the two edges of the ZGNR are characterized by opposite spin orientations and couple through the graphene backbone via an

M. S. Deleuze (✉) · M. Huzak  
Theoretical Chemistry and Molecular Modelling,  
Hasselt University,  
Agoralaan, Gebouw D,  
B-3590 Diepenbeek, Belgium  
e-mail: michael.deleuze@uhasselt.be

B. Hajgató  
General Chemistry Division, Member of the QCMM Research  
Group – alliance Ghent-Brussels, Free University of Brussels,  
Pleinlaan 2,  
B1050 Brussels, Belgium

antiferromagnetic arrangement of spins on adjacent atomic sites. The total spin ( $S$ ) is therefore identically equal to zero, which is in agreement with the implications of Lieb's theorem [23] for compensated bipartite lattices [24–27]. Reversing from condensed matter physics to the terminology employed in quantum chemistry, ZGNRs are thus considered to possess a (so-called) “singlet open-shell” electronic ground state characterized by symmetry-broken spin-densities, a view that spin-unrestricted DFT calculations with various exchange-correlation functionals on large enough but finite polycyclic aromatic hydrocarbons [28–32] (PAHs) also confirm.

Half-metallicity has been predicted for many related systems, comprising edge-oxidized, edge-reconstructed or doped graphene nanoribbons [33–35], zigzag single-walled carbon or hybrid BN-C nanotubes of finite width [36–38], and partially open armchair carbon nanotubes [39]. These predictions systematically find their roots into the results of (spin-unrestricted) DFT calculations and invariably the same constataion that spatially separated spin-up and spin-down Kohn-Sham orbitals are subject to opposite energy shifts when an external electric field is applied across the nanoribbon. Extended ZGNRs are thus considered nowadays to be highly promising materials with regards to *spintronics* (i.e. *spin transport electronics* [40]), a new technology where it is not the electric charge but the electron spin that carries information. By virtue of the resemblance of the spin-polarization (up or down) with the information zero or one in regular electronics, monitoring spin transports in appropriate materials offers opportunities for a new generation of devices combining microelectronics with spin-dependent effects due to interactions between the spin of the carrier and local magnetic fields. Devices such as spin-field effect transistors and light emitting diodes, spin resonant tunnelling devices, optical switches operating at terahertz frequency, modulators, encoders, decoders, or quantum bits for quantum computation and communication are already envisioned.

According to Hod *et al.*, and their study [32] based on DFT calculations employing the LSDA functional, the semi-local gradient corrected functional of Perdew, Burke, and Ernzerhof [41, 42] (PBE), and the screened exchange hybrid density functional due to Heyd, Scuseria, and Ernzerhof (HSE06) [43–45], the smallest hydrocarbon structures which possess antiferromagnetically ordered frontier edge states subject to a half-metallic spin-polarization in the presence of a transversal external electric field are  $C_{28}H_{14}$  (phenanthro[1,10,9,8-opqra]perylene, alias bisanthrene) and  $C_{36}H_{16}$  (tetrabenzo[bc,ef,kl,no]coronene (Fig. 1a,b). It has also recently been conjectured [46–53] that  $n$ -acenes larger than pentacene or hexacene (Fig. 1c,d) are “open-shell singlet” (i.e. *antiferromagnetic*) systems, resulting again quite logically in the conclusion that these systems become half-

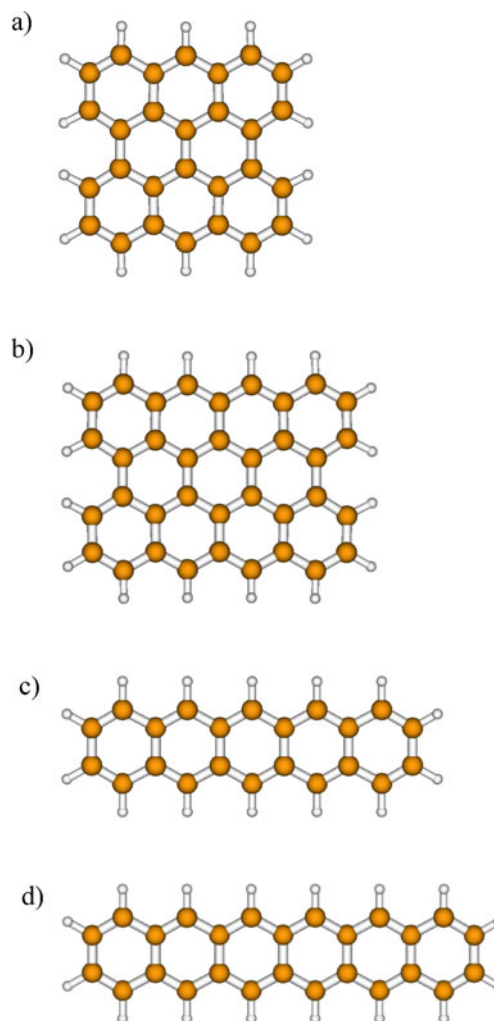


**Fig. 1** Molecular structures of **a** phenanthro[1,10,9,8-opqra]perylene, alias bisanthrene [ $C_{28}H_{14}$ ]; **b** tetrabenzo[bc,ef,kl,no]coronene [ $C_{36}H_{16}$ ]; **c** pentacene ( $n=5$ ); and **d** hexacene ( $n=6$ ).

metallic in the macroscopic limit [54],  $n \rightarrow \infty$ . At the UB3LYP/6-31G\* level of theory, [ $n$ ]cyclacenes were similarly found to have a spin-polarized open-shell wave function in their singlet ground state when  $n$  is greater than 5 [55]. In all these calculations upon finite molecular systems, an electronic (singlet) instability can be diagnosed from the fact that in unrestricted calculations, the two outermost singly occupied  $\alpha$  and  $\beta$  spin-orbitals deviate from the  $D_{2h}$  symmetry point group imposed by the nuclear frame, due to a *symmetry-breaking* in the form of a localization of the two frontier electrons on the two zig-zag edges.

A main conceptual difficulty at this stage is that symmetry-breakings of spin-densities in the singlet eigenstates of spin-free Hamiltonians violate well-established principles and basic theorems of quantum mechanics (*point group theory*, *spin quantization*). A *singlet* ground state in (large but finite) molecules with an even number ( $2N$ ) of electrons implies in particular that canonical orbitals have to transform according

to irreducible representations of the molecular symmetry point group [56, 57] and most strictly forbids any difference in between  $\alpha$ - and  $\beta$ - spin-densities. When  $S=0$ , whatever the fundamental band gap and the extent of the multi-reference character (i.e. bi- or polyradicalism) of the electronic wave function, each  $\alpha$  spin-orbital must possess a  $\beta$  partner with the same space function, and the spin-density must be identically zero at every point in space. In the absence of energy degeneracies, spin-orbitals in a singlet electronic state are symmetry-adapted, exactly paired, and the charge density is totally symmetric under the molecular symmetry point group. Therefore, when  $S=0$ , departures of spin-densities from the symmetry dictated by the Full Hamiltonian and by the nuclear framework are most clearly *artefactual* [58], i.e. due to an incomplete treatment of electron correlation [59, 60]. Even in the case of physical symmetry breakings, such as, typically, Jahn-Teller distortions of the molecular structure induced by energy degeneracies under non-abelian symmetry point groups [61, 62], only *electric* charges can localize if the wave function remains a *singlet*. If an unrestricted Self-Consistent Field (SCF) calculation upon a *singlet* wave function enforces different localizations for orbitals with opposite spin and an energy lowering into a so-called “singlet open-shell” ground state, a spin-contamination by (magnetically active) triplet, quintet... etc. states arises and provides a straightforward measure of the extent of the symmetry breaking [63]. Spin-orbit coupling interactions are at first glance intrinsically far too weak to provide any support to the idea of “*spontaneous*” and physical symmetry breakings in carbonaceous materials: their estimated effect on the band gap of graphene does not exceed  $24 \mu\text{eV}$  [64]. Note that, in their discussion of the spin-polarization of edge states of graphene islands of finite (nanometric) dimension, Rudberg *et al.* [29] already grasped that the half-metallic nature of ZGNRs should probably be an artefact of the employed DFT approaches.

Whereas Lieb’s theorem demonstrates that the total spin moment of graphene nanoribbons, graphene nanoislands and related extended or finite systems must be identically zero, the expectation value of the  $S^2$  operator is an important issue which has been so far altogether entirely neglected for these systems. The first purpose of the present contribution is to investigate the scaling properties with system size of this most important quantity, assuming that an antiferromagnetic depiction prevails for the singlet electronic ground state of model extended ribbons, as in the original *Nature*’s article by Son *et al.* [21]. In this purpose, we shall use the formalism [65–72] of crystalline orbitals for extended systems with periodicity in one-dimension (Fig. 2). It will be shown in particular that, in sharp contrast with the expected value (0) for the  $S^2$  operator in a singlet ( $S=0$ ) ground state, the spin contamination characterizing *any* UHF or UDFT wave function with symmetry-broken spin-densities has to diverge with the length of the ribbon, which formally

implies a complete loss of control upon spin-related properties in the macroscopic limit. Considering that symmetry-breakings of spin-densities can be enforced *at will on any conjugated compound by imposing too strong limitations on the employed wave function*, we will then resort to UHF calculations with a limited basis set to show that from its valence electronic structure even a small PAH compound like anthracene can exhibit features that are reminiscent of the half-metallicity of large but finite *Zig-zag Graphene NanoIslands* (ZGNIs). This conclusion will be tested again calculations employing larger basis sets, converging to the Complete Basis Set (CBS) limit, and many-body treatments of improving quality, in order to prove by analogy with larger systems and contradiction (*reductio ad absurdum*) of all available theoretical and experimental evidences for this compound that the half-metallicity of ZGNIs, ZGNRs, *n*-acenes and related systems will necessarily be quenched by an accurate enough treatment of electron correlation. The scaling properties of the spin contamination as a function of system size will also be investigated for the *n*-acene series, on the grounds of UHF and UDFT calculations, the latter in conjunction with a variety of functionals. We will thereby verify on computational grounds that half-metallicity in finite ZGNIs and extended ZGNRs is nothing else but a measure of the extent of an artefactual symmetry-breaking of spin-densities in spin-unrestricted one-determinantal (HF or DFT) calculations.

### Crystalline orbital analysis of spin-contamination in extended periodic chains

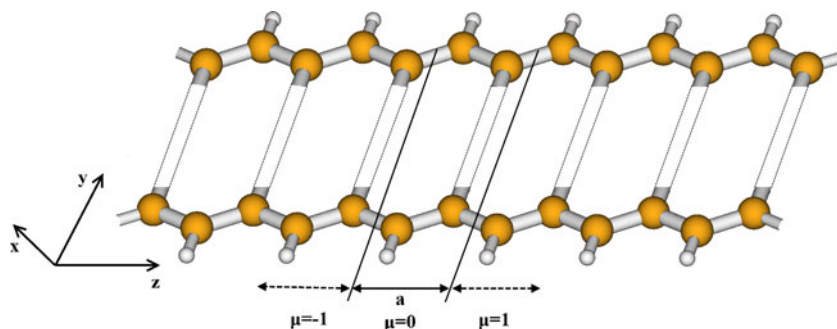
Any spin-unrestricted wavefunction (e.g. unrestricted HF, unrestricted B3LYP, LSDA, ...) for a given spin state is subject to contamination by higher-spin states, resulting in an expectation value for the  $S^2$  operator that exceeds the exact [ $S_z(S_z+1)$ ] value, because the contaminants have larger values of  $S$ . In particular, it is well-known that, for any single-determinantal spin-unrestricted UX wave function ( $X=HF, LSDA, B3LYP, \dots$ ), the  $\langle S^2 \rangle$  expectation value is of the form [59, 63]:

$$\langle S^2 \rangle_{UX} = S_z(S_z + 1) + N_\beta - \sum_{ij=1}^{MO} \langle \psi_i^\alpha | \psi_j^\beta \rangle^2 \quad (1)$$

From the above equation, it is clear that if the  $\alpha$  and  $\beta$  orbitals are identical in the singlet ( $S=S_z=0$ ) ground state, there is no spin contamination, and the unrestricted wave function is identical to the restricted one.

For an hypothetical singlet spin-polarized ground state in *n*-acenes or finite graphene nanoislands, the error in spin-contamination provides therefore a measure of the extent of the symmetry breaking:

**Fig. 2** CO-LCAO analysis of symmetry-breakings in extended ZGNRs and related systems with periodicity in one dimension



$$\langle S^2 \rangle_{UX} - \langle S^2 \rangle_{exact} = N_\beta - \sum_{i=1}^{N_\alpha} \sum_{j=1}^{N_\beta} \langle \psi_i^\alpha | \psi_j^\beta \rangle \langle \psi_j^\beta | \psi_i^\alpha \rangle \quad \langle S^2 \rangle_{UX} - \langle S^2 \rangle_{exact} = \Delta_1 \langle S^2 \rangle + \Delta_2 \langle S^2 \rangle \quad (10)$$

(2)

As usual, we assume an expansion of the spin-unrestricted molecular orbitals as a linear combination of  $K$  atomic functions  $\phi_p(\vec{r})$ :

$$\psi_i^\alpha(\vec{r}) = \sum_{p=1}^K C_{pi}^\alpha \phi_p(\vec{r}) \quad (3)$$

$$\psi_j^\beta(\vec{r}) = \sum_{q=1}^K C_{qj}^\beta \phi_q(\vec{r}) \quad (4)$$

under the usual orthonormality constraints for space functions relating to the same spin, i.e.

$$\mathbf{C}^{\alpha\dagger} \mathbf{S}^{\alpha\alpha} \mathbf{C}^\alpha = \mathbf{1} \quad (5)$$

$$\mathbf{C}^{\beta\dagger} \mathbf{S}^{\beta\beta} \mathbf{C}^\beta = \mathbf{1} \quad (6)$$

where

$$S_{ij}^{\alpha\alpha} = \langle \psi_i^\alpha | \psi_j^\alpha \rangle = \langle \psi_i^\beta | \psi_j^\beta \rangle = S_{ij}^{\beta\beta} = \delta_{ij} \quad (7)$$

Suppose:

$$\psi_j^\beta(\vec{r}) = \psi_j^\alpha(\vec{r}) + \delta_j(\vec{r}) \quad (8)$$

$$\psi_j^\beta(\vec{r}) = \sum_{q=1}^K (C_{qj}^\alpha + \Delta_{qj}) \phi_q(\vec{r}) \quad (9)$$

Upon taking the orthonormality of orbitals relating to the same spin function into account, we can decompose the spin contamination into first- and second-order contributions with regards to the spin-polarization  $\delta_j(\vec{r})$ :

along with:

$$\Delta_1 \langle S^2 \rangle = - \sum_{j=1}^N [(\langle \psi_j^\alpha | \delta_j \rangle + \langle \delta_j | \psi_j^\alpha \rangle)] \quad (11)$$

$$\begin{aligned} \Delta_2 \langle S^2 \rangle &= - \sum_{i=1}^N \sum_{j=1}^N \langle \psi_i^\alpha | \delta_j \rangle \langle \delta_j | \psi_i^\alpha \rangle \\ &= - \sum_{i=1}^N \sum_{j=1}^N |\langle \psi_i^\alpha | \delta_j \rangle|^2 \leq 0 \end{aligned} \quad (12)$$

Both contributions to the spin contamination identically cancel if  $\delta_j(\vec{r}) = 0$  for  $j=1, 2, \dots, N$ , and differ from zero otherwise. The second-order contribution  $\Delta_2$  in terms of the symmetry-breaking is obviously zero or negative. In contrast, further analysis demonstrates that the first-order term,  $\Delta_1$ , is necessarily zero or positive:

$$\begin{aligned} \Delta_1 \langle S^2 \rangle &= -2 \sum_{i=1}^N [\text{Re}(\langle \psi_i^\alpha | \delta_i \rangle)] \\ &= -2 \sum_{i=1}^N [\text{Re}(\langle \psi_i^\alpha | \psi_i^\beta \rangle - 1)] \geq 0 \end{aligned} \quad (13)$$

because

$$\text{Re}(\langle \psi_i^\alpha | \psi_i^\beta \rangle) \leq 1 \quad (14)$$

If the electronic ground state is a singlet, spin-contamination can only arise through admixture of states of higher spin-multiplicity (triplet, quintet, ...), and the spin contamination can therefore only be positive or equal to zero. For those situations where a symmetry-breaking in spin-densities prevails (i.e. when  $\delta_j(\vec{r}) \neq 0$ ), it is then clear that the first- and second-order contributions to spin-contamination can never exactly compensate:

$$\Delta_1 \langle S^2 \rangle \geq -\Delta_2 \langle S^2 \rangle \tag{15}$$

In order to adapt Eq. 11 to extended systems with periodicity in one dimension (Fig. 2), we now consider spin-unrestricted crystalline-orbitals (CO) of the form [65–72]:

$$\psi_n^\alpha(k, \vec{r}) = N_0^{-1/2} \sum_{\mu=1}^{N_0} e^{ik\mu a} \sum_{p=1}^K C_{pn}^\alpha(k) \phi_p^\mu(\vec{r}) \tag{16}$$

$$\psi_n^\beta(k, \vec{r}) = N_0^{-1/2} \sum_{\mu=1}^{N_0} e^{ik\mu a} \sum_{p=1}^K C_{pn}^\beta(k) \phi_p^\mu(\vec{r}) \tag{17}$$

where  $\phi_p^\mu(\vec{r})$  stands for an atomic function centered on atom  $p$  in cell  $\mu$ :

$$\phi_p^\mu(\vec{r}) = \phi_p(\vec{r} - \mu a \vec{e}_z - \vec{R}_p) \tag{18}$$

In Eqs. 16, 17,  $N_0$  represents the number of unit cells of width  $a$  of the extended periodic system, containing each  $K$  atomic functions, and assuming periodicity in one-dimension along the  $z$ -axis, under the usual (Born – Von Karman) constraint of cyclic boundary conditions [73].  $n$  and  $k$  stand for the band index and wave number (electron momentum), respectively. In straightforward analogy with Eq. 8, we correspondingly define crystalline spin-orbital differences as:

$$\begin{aligned} \delta_n(k, \vec{r}) &= \psi_n^\beta(k, \vec{r}) - \psi_n^\alpha(k, \vec{r}) \\ &= N_0^{-1/2} \sum_{\mu=1}^{N_0} e^{ik\mu a} \sum_{p=1}^K \Delta_{pn}(k) \phi_p^\mu(\vec{r}) \end{aligned} \tag{19}$$

$\psi_n^\alpha(k, \vec{r})$ ,  $\psi_n^\beta(k, \vec{r})$  and  $\delta_n(k, \vec{r})$  are obviously periodic functions that can be constructed as linear combinations of symmetry adapted functions, referred to as Bloch functions [74],  $u_p(k, \vec{r})$ :

$$\psi_n^\alpha(k, \vec{r}) = \sum_{p=1}^K C_{pn}^\alpha(k) u_p(k, \vec{r}) \tag{20}$$

$$\psi_n^\beta(k, \vec{r}) = \sum_{p=1}^K C_{pn}^\beta(k) u_p(k, \vec{r}) \tag{21}$$

$$\delta_n(k, \vec{r}) = \sum_{p=1}^K \Delta_{pn}(k) u_p(k, \vec{r}) \tag{22}$$

together with:

$$u_p(k, \vec{r}) = N_0^{-1/2} \sum_{\mu=1}^{N_0} e^{ik\mu a} \phi_p^\mu(\vec{r}) \tag{23}$$

Bloch functions are obtained from (atomic) functions  $\phi_p(\vec{r})$  without any particular symmetry by means of the projection operator [75]:

$$O_k = N_0^{-1} \sum_{\mu=1}^{N_0} e^{ik\mu a} \tag{24}$$

which has most important properties [76]:

$$O_k O_{k'}^\dagger = \delta(k, k') O_k \tag{25}$$

$$O_k^\dagger = O_k \tag{26}$$

Bloch functions are therefore necessarily block-diagonal in  $k$ :

$$\langle \psi_n^\alpha(k) | \psi_{n'}^\alpha(k') \rangle = \langle \psi_n^\beta(k) | \psi_{n'}^\beta(k') \rangle = \delta_{nn'} \delta(k, k') \tag{27}$$

Another important and well-known consequence of translation symmetry is periodicity of the electronic structure in the reciprocal ( $k$ ) space [77], whose elementary unit cell defines the first Brillouin zone (BZ), ranging from  $-\pi/a$  to  $+\pi/a$ . For the sequel, it is essential to remind that if the super-cell contains  $N_0$  unit cells, there can be only  $N_0$  possible discrete values of  $k$  in the first Brillouin zone. Each of these values corresponds to a specific irreducible representation of the translational symmetry point group, containing  $K$  spin-up and  $K$  spin-down Bloch functions characterized by their band index  $n=1, 2, 3, \dots, K$ .

In the macroscopic limit of an infinite system with finite densities, one most customarily makes use of the equivalence:

$$\lim_{N_0 \rightarrow \infty} \frac{1}{N_0} \sum_{\mu=1}^{N_0} \Leftrightarrow \frac{a}{2\pi} \int_{-\pi/a}^{+\pi/a} dk \tag{28}$$

Expanding the first-order contribution to spin contamination in terms of crystalline spin-orbitals, and carrying out lattice summations, we get:

$$\begin{aligned} \Delta_1 \langle S^2 \rangle &= - \sum_n \sum_k^{BZ} [(\langle \psi_n^\alpha(k) | \delta_n(k) \rangle + \langle \delta_n(k) | \psi_n^\alpha(k) \rangle)] \tag{29} \\ &= \frac{-1}{N_0} \sum_n \sum_k^{BZ} \sum_{\mu, \mu'=1}^{N_0} e^{ik(\mu' - \mu)a} \sum_{pq=1}^K \\ &\quad (C_{pn}^{\alpha*}(k) \Delta_{qn}(k) S_{pq}^{\mu\mu'} + C_{pn}^\alpha(k) \Delta_{qn}^*(k) S_{pq}^{\mu\mu'*}), \end{aligned}$$

together with

$$S_{pq}^{\mu\mu'} = \langle \phi_p^\mu | \phi_q^{\mu'} \rangle \tag{30}$$



Considering that

$$S_{pq}^{\mu\mu'} = S_{pq}^{0\mu''}; \mu'' = \mu' - \mu; \tag{31}$$

and

$$\sum_{\mu,\mu'=1}^{N_0} \Leftrightarrow N_0 \sum_{\mu''=1}^{N_0}; \tag{32}$$

it follows that, by exploiting translation symmetry, Eq. 29 reduces to:

$$\Delta_1 \langle S^2 \rangle = - \sum_n \sum_k^{BZ} \Gamma_n(k), \tag{33}$$

together with:

$$\Gamma_n(k) = \sum_{\mu''=1}^{N_0} e^{ik\mu''a} \sum_{pq=1}^K \left( C_{pn}^{\alpha*}(k) \Delta_{qn}(k) S_{pq}^{0\mu''} + C_{pn}^{\alpha}(k) \Delta_{qn}^*(k) S_{pq}^{0\mu''*} \right) \tag{34}$$

$\Gamma_n(k)$  obviously remains a finite bounded function in the macroscopic limit  $N_0 \rightarrow \infty$ , since successive terms in the lattice summation decay exponentially with  $\mu''$  [78–82], as the overlap between the atomic functions  $\phi_p^0(\vec{r}) = \phi_p(\vec{r} - \vec{R}_p)$  and  $\phi_q^{\mu''}(\vec{r}) = \phi_p(\vec{r} - \mu''a\vec{e}_z - \vec{R}_q)$ . Since there are only  $N_0$  possible discrete values of  $k$  in the first BZ, it is clear therefore that, in the macroscopic limit, the first-order contribution to spin-contamination has to scale proportionally to the number of unit cells in the periodic system. Indeed, because of the equivalence (28), Eq. 33 yields:

$$\lim_{N_0 \rightarrow \infty} \Delta_1 \langle S^2 \rangle = -N_0^{+1} \frac{a}{2\pi} \int_{-\pi/a}^{+\pi/a} \left( \sum_n \Gamma_n(k) \right) dk \tag{35}$$

We now consider an adaptation to crystalline orbitals for extended periodic chains of the second-order contribution to spin-contamination, and find, similarly:

$$\begin{aligned} \Delta_2 \langle S^2 \rangle &= - \sum_{n,n'} \sum_{k,k'}^{BZ} \langle \psi_n^{\alpha}(k) | \delta_{n'}(k') \rangle \langle \delta_{n'}(k') | \psi_n^{\alpha}(k) \rangle \\ &= - \sum_{n,n'} \sum_k^{BZ} \langle \psi_n^{\alpha}(k) | \delta_{n'}(k) \rangle \langle \delta_{n'}(k) | \psi_n^{\alpha}(k) \rangle \\ &= \frac{-1}{N_0^2} \sum_{n,n'} \sum_k^{BZ} \sum_{\mu_1,\mu_2=1}^{N_0} \sum_{\mu_3,\mu_4=1}^{N_0} e^{ik(\mu_2+\mu_4-\mu_1-\mu_3)a} \\ &\quad \times \sum_{pqrs=1}^K C_{pn}^{\alpha*}(k) \Delta_{qn'}(k) \Delta_{rn'}^*(k) C_{sn}^{\alpha}(k) S_{pq}^{\mu_1\mu_2} S_r^{\mu_3\mu_4} \end{aligned} \tag{36}$$

Again, because of the periodicity of the lattice, we can exploit the following relationships:

$$\begin{aligned} S_p^{\mu_1\mu_2} &= S_{pq}^{0\mu'} \\ S_r^{\mu_3\mu_4} &= S_r^{\mu''0} = S_s^{0\mu''*} \end{aligned} \tag{37}$$

where  $\mu' = \mu_2 - \mu_1$  and  $\mu'' = \mu_3 - \mu_4$  along with the equivalences

$$\begin{aligned} \sum_{\mu_1,\mu_2=1}^{N_0} &\Leftrightarrow N_0 \sum_{\mu'=1}^{N_0} \\ \sum_{\mu_3,\mu_4=1}^{N_0} &\Leftrightarrow N_0 \sum_{\mu''=1}^{N_0} \end{aligned} \tag{38}$$

This enables us to rewrite the second-order contribution to spin-contamination as follows:

$$\begin{aligned} \Delta_2 \langle S^2 \rangle &= - \sum_{n,n'} \sum_k^{BZ} \sum_{\mu',\mu''=1}^{N_0} e^{ik(\mu'-\mu'')a} \sum_{pqrs=1}^K \\ &\quad \left( C_{pn}^{\alpha*}(k) \Delta_{qn'}(k) \Delta_{rn'}^*(k) C_{sn}^{\alpha}(k) S_{pq}^{0\mu'} S_{rs}^{0\mu''*} \right) \\ &= - \sum_{n,n'} \sum_k^{BZ} \sum_{\mu',\mu''=1}^{N_0} e^{ik(\mu'-\mu'')a} \sum_{pqrs=1}^K C_{pn}^{\alpha*}(k) \Delta_{qn'} \\ &\quad (k) S_{pq}^{0\mu'} C_{rn}^{\alpha}(k) \Delta_{sn'}^*(k) S_{rs}^{0\mu''*} \end{aligned} \tag{39}$$

Again, each term in the lattice summations over  $\mu'$  and  $\mu''$  decays exponentially as the charge distributions  $\gamma_p^{0*}(\vec{r})$ ,  $\gamma_q^{\mu'}(\vec{r})$  and  $\gamma_r^{0*}(\vec{r})$ ,  $\gamma_s^{\mu''}(\vec{r})$ , and these summations therefore both have to converge to a finite value in the macroscopic limit  $N_0 \rightarrow \infty$ . We thus define:

$$\lambda_{n,n'}(k) = \sum_{\mu'=1}^{N_0} e^{ik\mu'a} \sum_{pq=1}^K C_{pn}^{\alpha*}(k) \Delta_{qn'}(k) S_{pq}^{0\mu'} \tag{40}$$

and correspondingly:

$$\lambda_{n,n'}^*(k) = \sum_{\mu''=1}^{N_0} e^{-ik\mu''a} \sum_{rs=1}^K C_{rn}^{\alpha}(k) \Delta_{sn'}^*(k) \left( S_{rs}^{0\mu''} \right)^* \tag{41}$$

and find therefore that, in the macroscopic limit, the second-order contribution to spin-contamination has also to scale proportionally to system size:

$$\lim_{N_0 \rightarrow \infty} \Delta_2 \langle S^2 \rangle = -N_0^{+1} \frac{a}{2\pi} \int_{-\pi/a}^{+\pi/a} \left( \sum_{n,n'} |\lambda_{n,n'}(k)|^2 \right) dk \tag{42}$$

Since the first-order and second-order contribution cannot exactly compensate (except if they both identically vanish, i.e. in the absence of spin-symmetry breakings), a most important result of this analysis is that, for any unrestricted single-determinantal treatment (UHF, LSDA, UB3LYP, ...) which results into a net transversal spin-polarization, the spin-contamination of the electronic ground state of  $n$ -acenes and extended graphene nanoribbons of finite width and periodicity into one dimension has to scale proportionally to the length of

the ribbon ( $N_0$ ), and to diverge therefore to a positive infinite value in the macroscopic limit ( $N_0 \rightarrow \infty$ ). This conclusion is obviously in most striking contradiction with the implications of Lieb's theorem for compensated bipartite lattices and with the normal expectation for a singlet electronic ground state ( $S=0$ , and thus,  $\langle S^2 \rangle = 0$ ).

$$\begin{aligned} \lim_{N_0 \rightarrow \infty} \langle S^2 \rangle_{UX} - \langle S^2 \rangle_{exact} & \quad (43) \\ &= -N_0^{+1} \frac{a}{2\pi} \int_{-\pi/a}^{+\pi/a} \sum_n \left[ \Gamma_n(k) + \sum_{n'} |\lambda_{n,n'}(k)|^2 \right] dk \\ &= +K N_0^{+1} \end{aligned}$$

In the above equation, the constant  $K$  is a finite scaling factor which depends on the characteristics of the model nanoribbon and employed exchange-correlation functionals and basis sets. This constant is identically 0 in the absence of symmetry-breaking in spin-densities (i.e. when  $\delta_n(k, \vec{r}) = 0 \forall n = 1, 2, \dots, K; \forall k \in BZ$ ).

### Methodology and computational details

All calculations on  $n$ -acenes that are presented in this work have been carried out using the GAUSSIAN09 package of programs [83], on field-free geometries that were all optimized according to restricted DFT calculations employing the Becke-3-parameters-Lee-Yang Parr functional (B3LYP [84, 85]) along with Dunning's correlation consistent polarized valence basis set of triple zeta quality (cc-pVTZ), under the constraint of the topologically required  $D_{2h}$  symmetry point group [86–88]. We then apply the UHF approach upon these geometries, in order to *enforce* a symmetry-breaking of spin-densities (i.e. a spin-polarization of edge states) at the onset of the  $n$ -acene series (benzene, naphthalene, ...) and in the absence of any external perturbation, and verify the scaling properties of the spin contamination. Comparison is made with spin-unrestricted DFT calculations employing a variety of functionals, comprising the gradient corrected Becke-Lee-Yang-Parr (BLYP) functional, the hybrid Becke-3-parameters-Lee-Yang-Parr (B3LYP) [84, 85] functional, and the Modified 1-parameter Perdew-Wang functional for kinetic (MPW1K [89, 90]), as well as the double hybrid dispersion corrected B2PLYPD [91] functional. The MPW1K functional is a modification of the MPW1PW91 (modified Perdew-Wang 1991 Perdew Wang) functional [92] with an increase fraction of HF versus DFT exchange (0.428:0.572 instead of 0.25:0.75). This functional has been specifically designed for handling situations where HF exchange dominates because of enhanced electron delocalization, as for instance in transition states on chemical reaction pathways.

We then illustrate with anthracene the consequences of symmetry-breakings in spin-densities at the UHF level when an external electric field is progressively switched on, using the Finite Field approach [93–101] and using basis sets of improving quality (STO-3G [63], 6-31G [63], 6-31G\*\* [63], cc-pVXZ ( $X=T, Q, 5, \infty$ ) [102]). Results obtained using Dunning's correlation consistent polarized valence basis sets [cc-pVXZ] are extrapolated to the limit of an asymptotically complete basis set [ $X=\infty$ ] using Feller's formula [103, 104]. We then evaluate for this compound the influence of the external field on symmetry-broken (i.e. unrestricted) and symmetry-restricted spin-densities at varying orders in electron correlation, according to single-point calculations employing the same reference (RB3LYP/cc-pVTZ) geometry and STO-3G basis set, at the level of Møller-Plesset theory [105] truncated at second-order (MP2) [106, 107], third-order (MP3) [106], and fourth order with Single, Double and Quadruple excitations (MP4SDQ) [108], as well as Coupled Cluster Theory along with Single, Double or Single, Double and perturbative Triple excitations, shortly CCSD or CCSD(T) [109–112].

At this stage, it is useful to remind that anthracene has a relatively large band gap and sizeable electronic excitation energies. The vertical singlet-triplet energy gap of anthracene amounts for instance to  $56.9 \text{ kcal mol}^{-1}$  (2.46 eV) [113]. There is therefore a consensus on the fact that anthracene is a closed-shell non-magnetic (more specifically paramagnetic) system that can be very reliably described by single-reference approaches (see e.g. Ref. 16b). No symmetry constraint was enforced when the external electric field was applied perpendicularly to the zig-zag edges of the  $n$ -acenes and selected ZGNRs, i.e. along the  $y$ -axis (Fig. 2) in the standard orientation defined according to the usual conventions [114] for a molecule exhibiting a  $D_{2h}$  point group.

### Results and discussion

Size-dependence of spin contamination and of half-metallic spin-orbital energy-splits in model  $n$ -acenes

As was to be expected from the CO-LCAO analysis of the preceding section, we find (Fig. 3) from our calculations on model  $n$ -acenes ( $n=1-11$ ) that, with all selected functionals (including the HF approach),  $\langle S^2 \rangle$  becomes linearly dependent upon the number of unit cells ( $n$ ) in the system, when this number becomes large enough. At the UHF/6-31G level, the onset of the symmetry breaking in spin-densities lies at the origin of the  $n$ -acenes series (benzene, naphthalene), and the scaling in size of the spin contamination is therefore perfectly linear. The onset of the symmetry-breaking lies at the level of naphthalene ( $n=4$ ), hexacene

( $n=6$ ) and octacene ( $n=8$ ) with the MPW1K, B3LYP and BLYP functionals, respectively. A singlet instability and spin-polarization into a “singlet open-shell” wave function is also observed when  $n \geq 4$  with the SCF wave function employed in the B2PLYPD model. Note that, for all systems, at the B2PLYPD/6-31G level, the energy-order reverses in favor of the singlet closed-shell electronic ground state when the second-order (MP2-like) correlation energy is added to the obtained SCF (HF-like) energy. These numerical fits and observations confirm that, whenever a non-vanishing symmetry-breaking in spin-densities is detected in each unit cell,  $\langle S^2 \rangle$  has to diverge proportionally to system size in the macroscopic limit. Therefore, unless one wants to call Lieb’s theorem into question and its implications for compensated bipartite lattices, we can already conclude that, when assuming a singlet electronic ground state, an antiferromagnetic ordering and, thus, a half-metallic spin-polarization of edge states in perfectly regular ZGNRs and related systems are mathematically ruled out in the framework of non-relativistic time-independent many-body quantum mechanics, and in the absence of complications such as magnetic perturbations, in particular spin-orbit interactions. In other words, the main conclusions of the Nature’s paper by Louie, Cohen and Son [21] and of many related papers [33–39] appear to be nothing else that the outcome of a most common methodological artefact, which is quite

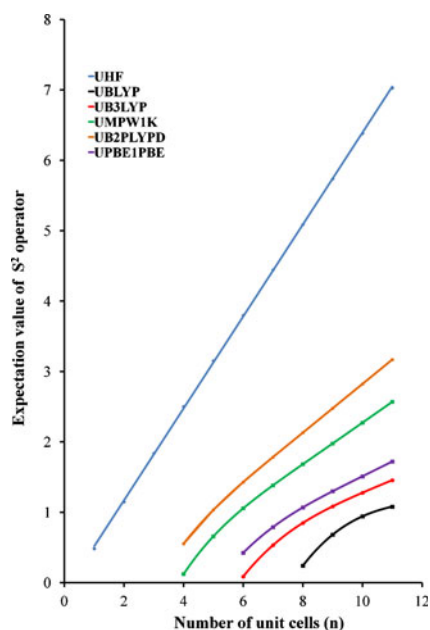


**Fig. 3** Evolution of the spin-contamination as a function of the length of the ribbon ( $n$ ) in the  $n$ -acenes [ $2 \times n$ ] series (results obtained using various exchange-correlation functionals along with the 6-31G basis, upon RB3LYP/cc-pVTZ geometries)

well understood in a quantum chemical framework, but has been most commonly ignored within the framework of solid state physics and band structure calculations.

In Fig. 4, we display at the UHF/6-31G and UHF/6-31G\*\* levels the split in energy of spin-up ( $\alpha$ ) and spin-down ( $\beta$ ) frontier orbitals (HOMO, LUMO) in function of the strength of the applied transversal electric field and number of monomer units in the  $n$ -acene ribbon. For all systems, this split slightly decreases upon improving the basis set. Whatever the basis set, it is directly proportional to the external field, and grows monotonically (logarithmically) with  $n$ . This growth is directly imputable to the decreasing HOMO-LUMO band gap with increasing system size, which results into an enhancement of the propensity of the electronic wave function to undergo a symmetry-breaking in the underlying spin-densities. Indeed, in symmetry breaking situations, because of the non-analytic (i.e. iterative) nature of solutions obtained with any self-consistent field (HF, DFT, mean field Hubbard or even CASSCF) procedure, the equation that governs the convergence of expansion coefficients is of the form [115, 116]:

$$(\varepsilon_\mu - \varepsilon_n) C_{\mu n}^{(q)} + \sum_{k=1}^N \sum_v [\langle \mu v | nk \rangle + \langle \mu k | nv \rangle] C_{vk}^{(q)} = D_{\mu n}^{(q)} \quad (44)$$

where  $\langle \alpha \beta | ij \rangle$  and  $\varepsilon_\alpha$  stand for anti-symmetrized bielectron integrals and orbital energies, respectively. In the above equation,  $q$  denotes the order of the change in the orbitals and in the associated energies, according to a one-electron perturbation expansion with respect to an infinitesimally small geometrical variation. For small nuclear displacements, the first-order driving term  $D_{\mu n}^{(1)}$  relates to minus the gradient of the electron-nuclei attraction potential in the direction of the symmetry-breaking transformation. Since Hamiltonian operators are necessarily Hermitian,  $C_{\mu n}^{(q)}$  is equal to  $(-C_{n\mu}^{(q)})$  in any SCF (HF, DFT, or even CASSCF) procedure, and only occupied – non occupied elements of the  $C^{(q)}$  matrix effectively contribute to the SCF energy [116]. Therefore, because of the energy-dependence of the first term on the left hand side of Eq. 44, it is clear that the convergence of orbital expansion coefficients in SCF calculations becomes particularly problematic in the event of near energy degeneracies between occupied and unoccupied levels. If the band gap vanishes, tiny distortions in orbital symmetries resulting for instance



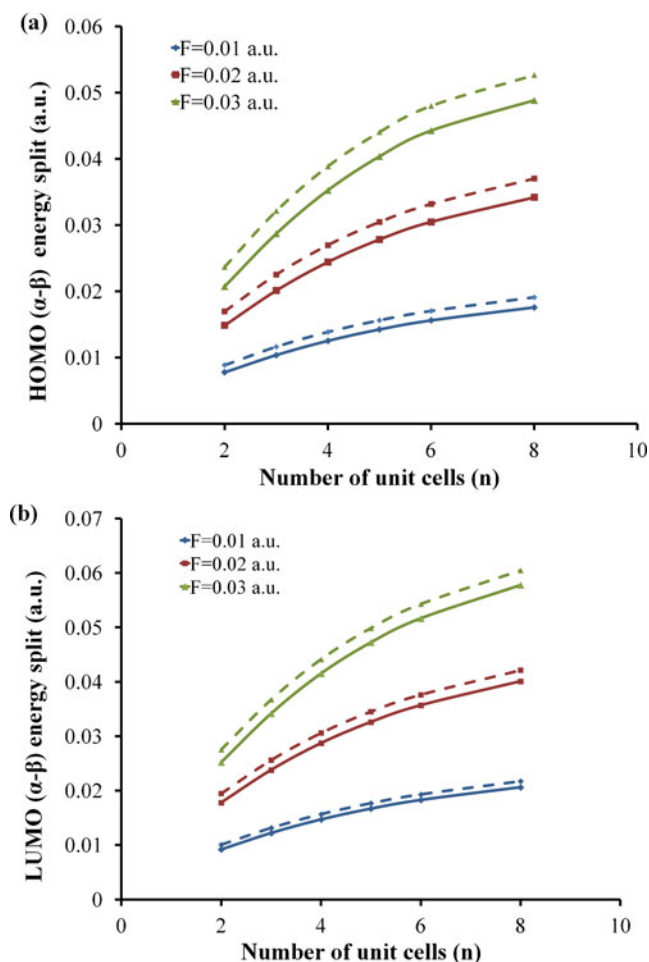


**Fig. 4** Evolution of the energy split of frontier orbitals due to the symmetry-breaking of spin-densities in function of the applied external electric field. Full and dashed lines refer to results obtained using the 6-31G\*\* and 6-31G basis sets, respectively

from any infinitesimally small nuclear displacements or numerical errors may amplify during the SCF iterations and can ultimately result into an asymptotically diverging energy lowering. A full divergence will be nonetheless avoided in the macroscopic limit, because any symmetry breaking in spin-densities precisely results into an opening of the fundamental band gap, preventing therefore real degeneracies to occur.

**Anthracene: an antiferromagnetic and half-metallic graphene nanoisland?**

In straightforward analogy with the work by Hod *et al.* on bisanthrene [32], we compare in Fig. 5 RHF/STO-3G and UHF/STO-3G levels contour plots of the frontier spin-orbitals of anthracene as a function of the external field. The evolution with the field of valence spin-orbital energies is correspondingly given at the UHF/STO-3G level in Fig. 6. With both figures, the resemblance with the results

obtained in ref. 32 for bisanthrene using a variety of exchange-correlation functionals and basis sets is most striking. In the absence of an external field, symmetry-broken  $\alpha$  and  $\beta$  UHF spin-orbitals (Fig. 5) have identical energies (Fig. 6). Due to the different space localization and polarization by the external electric field of unrestricted  $\alpha$  and  $\beta$  spin-densities (Fig. 5), energy degeneracies between spin band systems are released when applying an external field in the plane and across the longitudinal axis of the molecule (Fig. 6). Energy splittings due to the symmetry breaking are most striking for the  $\pi$ -levels, and barely noticeable for the  $\sigma$ -levels. At low electric fields ( $F < 0.025$  a.u. [ $1 \text{ a.u.} = E_h e^{-1} a_0^{-1} = 5.142 \cdot 10^{11} \text{ V m}^{-1}$ ]), we observe an increase of the fundamental (HOMO-LUMO) gap in one spin (say  $\alpha$ ) band system, and conversely a decrease of the HOMO-LUMO gap in the opposite ( $\beta$ ) spin-band system (Fig. 7a). Pursuing towards larger values of the field, we observe overall a destabilization of the occupied  $\pi$  and  $\sigma$  levels, and conversely a stabilization of the unoccupied  $\pi$  and  $\sigma$  levels of anthracene (Fig. 6). Also, both at the UHF/6-31G and UHF/6-31G\*\* levels, fields comprised between  $\sim 0.08$  and  $\sim 0.1$  a.u. prevent any symmetry-breaking in spin-densities, resulting in a  $\langle S^2 \rangle$  value equal to zero (Fig. 7b). Energy degeneracies between the  $\alpha$  and  $\beta$  spin band systems correspondingly disappear (Fig. 8).

As a continuous decrease of  $\langle S^2 \rangle$  in function of the field demonstrates (Fig. 7b), the external field tends to attenuate the symmetry-breaking in spin-densities and the energy splits of spin-up and spin-down orbitals, until reaching values comprised between  $\sim 0.075$  and  $\sim 0.1$  a.u. . At these latter values, at the UHF/6-31G and UHF/6-31G\*\* levels, a restricted closed-shell depiction prevails since  $\langle S^2 \rangle = 0$ . The strongest differences in orbital topologies and spreads are quite naturally therefore observed at zero field (Fig. 5). Further examination of the  $\langle S^2 \rangle$  values and of the UHF/6-31G\*\* spin-orbital energies displayed in Figs. 7b and 8 demonstrates that improving the basis set helps to reduce the extent of the symmetry-breaking in the spin-densities of anthracene at low external fields ( $F < 0.075$  a.u.). Note correspondingly that at zero field, spin-polarizations and energy lowering into a singlet open-shell electronic wave function occur at the UHF level, irrespective of the employed basis set: see in Fig. 9 the evolution of the difference between the RHF and UHF energies obtained in conjunction with basis sets of increasing size, among which Dunning's correlation consistent polarized valence basis sets of triple-, quadruple- and pentuple-zeta quality, along with the corresponding estimate in the limit of an asymptotically complete (cc-pV $\infty$ Z) basis set, according to an extrapolation employing Feller's formula. From this latter figure, it is clear that a symmetry-breaking of spin-densities remains in this limit, in the absence of an external electric field, and is

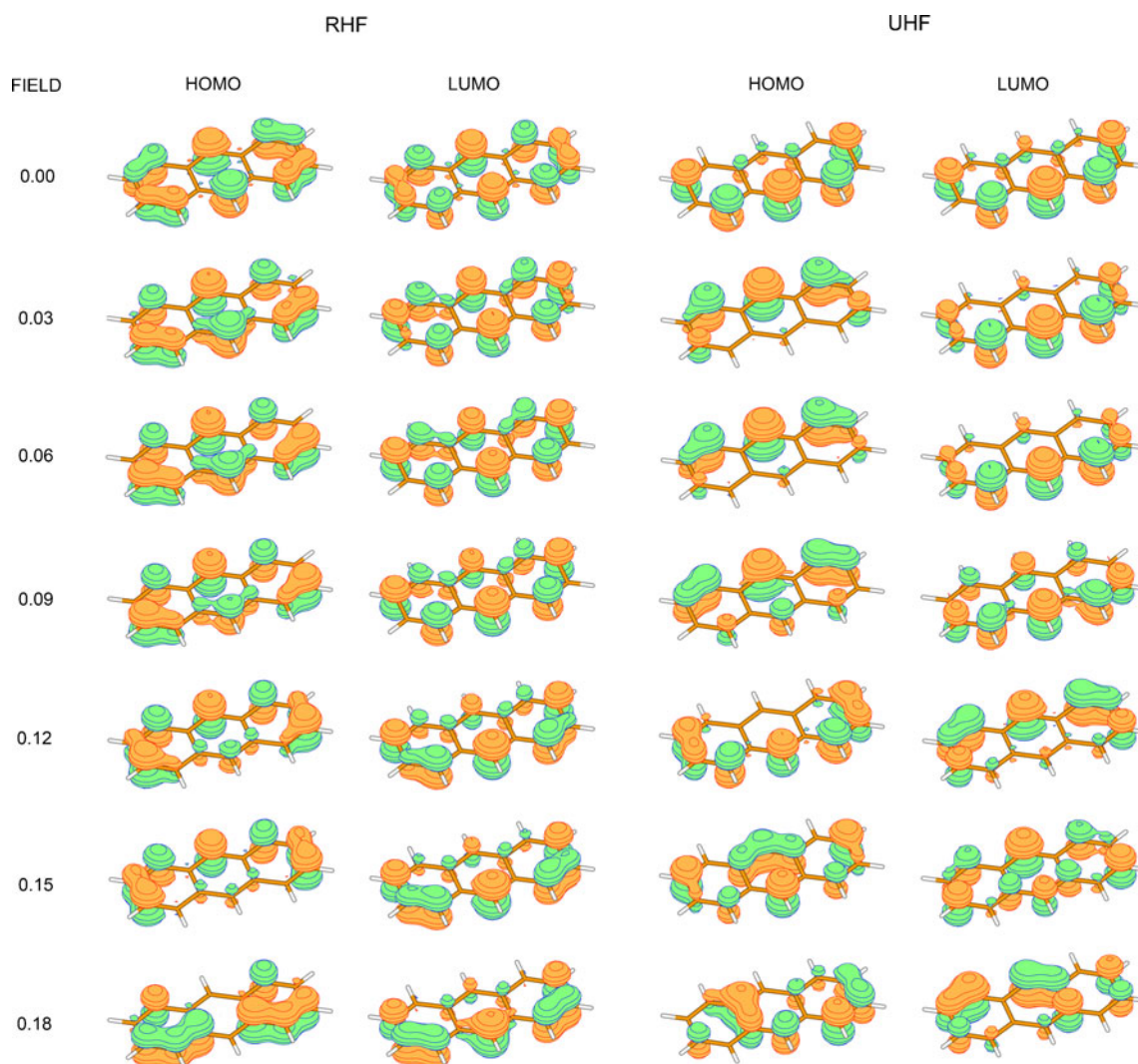


**Fig. 5** Evolution of the frontier spin-orbitals (HOMO, LUMO) of anthracene in function of the applied external electric field (in a.u.) at the RHF/STO-3G and UHF/STO-3G levels (results obtained using the same field free RB3LYP/cc-pVTZ reference geometry)

thus before all the outcome of a too approximate treatment of electron correlation.

Note that the largest values we consider for the electric field are exceedingly strong and may in practice exceed the dielectric strength of anthracene, leading to a cascade of electrons and a field ionization, if not a destruction of the molecule. This does not occur in our simulations, because of the limitations in the employed basis set. Field ionization is more likely to occur when applying a transversal electric field onto extended graphene nanoribbons, due to the vanishing band gap and extreme polarizabilities of these systems in the macroscopic limit.

#### Symmetry-breakings and symmetry-restorings

In view of singlet-triplet energy gaps of the order of  $56.9 \text{ kcal mol}^{-1}$  (2.47 eV) [112] and  $25.0 \text{ kcal mol}^{-1}$  (1.08 eV) [117] for anthracene and bisanthrene, respectively,

it is clear that for these two compounds any symmetry-breakings of spin-densities and stabilization of the electronic wave function into a singlet open-shell state must be regarded as artefactual. Such energy differences are far too large to be superseded by thermal fluctuations ( $kT=0.6 \text{ kcal mol}^{-1}$  at 298 K) or magnetic perturbations due for instance to C-13 nuclei, in the Mhz range [118, 119]. If we reason by contradiction (*reductio ad absurdum*), it makes sense to state that, at the UHF level, anthracene is one of the *smallest* possible examples of an *anti-ferromagnetic* (i.e. singlet open-shell) zig-zag graphene nanoisland exhibiting edge states subject to half-metallic spin-polarizations by an external field. The fact that anthracene is notoriously known as a single reference closed-shell and paramagnetic system most obviously demonstrates the inconvenience of such a statement. Proceeding further by contradiction of well-established experimental evidences, it is also worth mentioning that a spin-polarization of the singlet electronic ground state can be enforced *at will* for

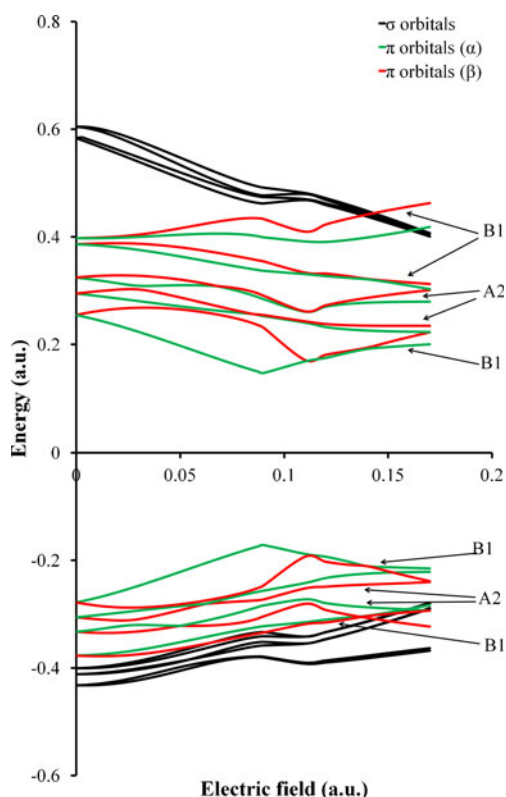


**Fig. 6** Evolution of the UHF/STO-3G energies of valence and unoccupied molecular spin-orbitals of anthracene. Symmetry labels for  $\pi$ -orbitals are consistent with the effective  $C_{2v}$  point when symmetry is reduced by the external field (results obtained using the same field free RB3LYP/cc-pVTZ reference geometry)

*any conjugated molecule* by resorting to a too inaccurate treatment of electron correlation with single-determinantal approaches. For instance, at the UHF/6-31G level, spin-polarization of the singlet closed-shell (spin-restricted) ground state of 1,3-butadiene, benzene and biphenyl into a singlet open-shell (spin-unrestricted) states yields spurious energy lowerings by 3.34, 2.36 and 7.30 kcal mol<sup>-1</sup>, at the expense of a spin-contamination equal to 0.4781, 0.4947 and 1.1561, respectively (results obtained using RB3LYP/cc-pVTZ geometries).

For a singlet electronic ground state, whatever the band gap and extent of the polyradicaloid (i.e. multireference) character of the wave function, symmetry breakings in spin-densities are necessarily the outcome of too approximate treatment of electronic correlation. To illustrate this point further, we display in Table 1 the evolution in function of the field of the energy differences between the spin-unpolarized singlet closed-shell and symmetry-broken “singlet open-shell” states of anthracene, at improving levels in the treatment of (dynamic) electron correlation by means of many-body quantum mechanics, within the framework of single-reference (i.e. single-determinantal) approaches. These comprise Hartree-Fock (HF) theory, Møller-Plesset

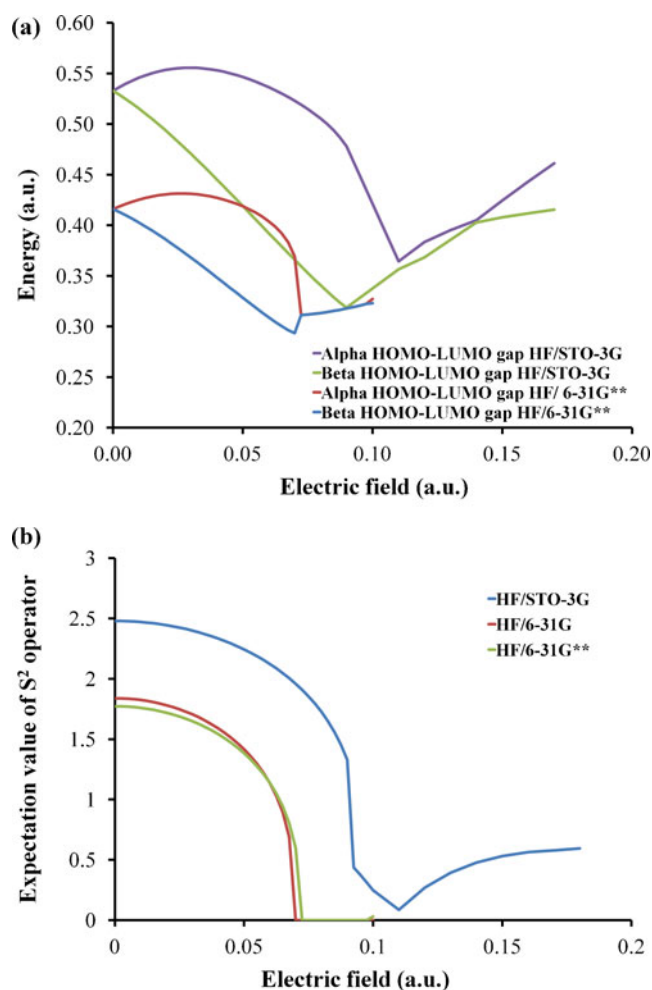


**Fig. 7** Evolution of **a** the fundamental energy gaps in the  $\alpha$ - and  $\beta$ -spin-band systems and **b** the UHF expectation value of the  $S^2$  operator (UHF results obtained for anthracene, using the field free RB3LYP/cc-pVTZ reference geometry)

perturbation theory [105] truncated at second-order, third-order and partial fourth-order (MP2 [106, 120], MP3 [106, 121], MP4SQD [106]), Coupled Cluster theory [110, 122, 123] with single and double excitations (CCSD), and CCSD theory supplemented by perturbative triple excitations (CCSD(T)). We note that since these methodological levels slowly converge to a full-CI depiction representing the exact solution of the electronic Schrödinger equation in the selected basis set, they also somehow indirectly recover the static correlation which is traditionally ascribed to near-energy degeneracies, i.e. multi-reference effects. Whatever the basis set, Fermi correlation at the UHF level most systematically overemphasizes the biradical character of the wave function, resulting in a “singlet open-shell” state which is located several tenths kcal mol<sup>-1</sup> below the proper singlet closed-shell state. Also, whatever the employed basis set and applied external field, the energy order always reverses in favour of the restricted wave functions with



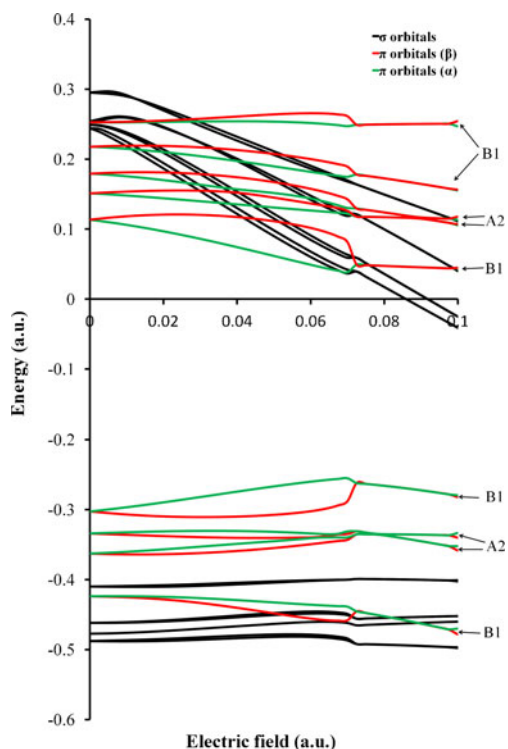


**Fig. 8** Evolution of the UHF/6-31G\*\* energies of the molecular spin-orbitals of anthracene as a function of the applied electric field. Symmetry labels for  $\pi$ -orbitals are consistent with the effective  $C_{2v}$  point group when symmetry is reduced by the external field (results obtained using the same field free RB3LYP/cc-pVTZ reference geometry)

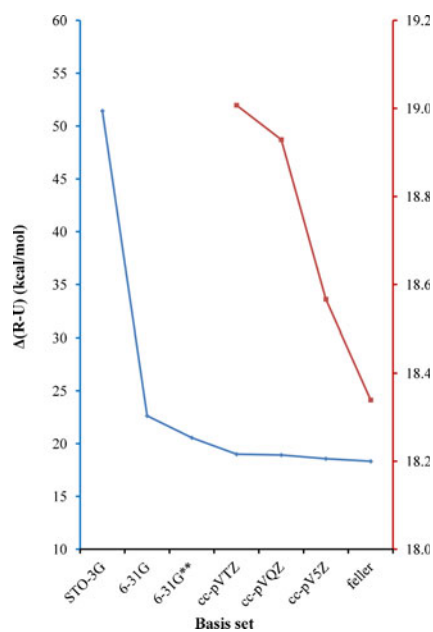


**Fig. 9** Evolution of the energy difference (in  $\text{kcal mol}^{-1}$ ) between the RHF and UHF wave functions of anthracene upon using basis sets of increasing size and converging to the limit of an asymptotically complete basis set. The red and blue axes correspond to results displayed in red and blue, respectively

spin-unpolarized orbitals when including dynamic electron correlation at the UMP2 and higher levels. This observation numerically illustrates the statement that symmetry-breakings and half-metallic spin-polarizations in spin-unrestricted calculations upon singlet states are necessarily the outcome of a too approximate treatment of *symmetry-restoring* electron correlation.

Similar considerations prevail within the framework of Density Functional Theory. For instance, within the framework of the UB2PLYPD model, if a singlet instability and intrinsic propensity for a spin-polarization of edge states can be diagnosed for the SCF wave function of  $n$ -acenes larger than anthracene (Table 2), the final energy order always reverse in favour of the closed-shell non-magnetic (spin-unpolarized) solution when non-local dynamic electron correlation is added to the hybrid functional by means of second-order perturbation theory. If double hybrid functionals were originally designed [124] for enabling more quantitative insights into heats of formation and reactions energies than standard hybrid functionals by a treatment of long-range dynamic correlation involving unoccupied orbitals, a quite unexpected advantage of these functionals is that they also most clearly increase the resilience of Density Functional Theory against artefactual symmetry breakings. Since both the SCF and second-order corrections to the (U-R) energy difference become proportional to the length of the ribbon when  $n$  becomes large enough, it is clear that, in the macroscopic limit ( $n \rightarrow \infty$ ), the most stable wave function will correspond to a closed-shell depiction at the B2PLYPD/6-31G level.

## Conclusions and outlook for the future

The greatest care is advocated with the currently prevailing view that zig-zag graphene nanoribbons and nanoislands of large enough dimensions exhibit antiferromagnetically ordered edge states subject to a half-metallic spin-polarization, when an external electric field is applied perpendicularly to the edges. Indeed, it has been demonstrated and computationally verified for various exchange-correlation functionals that any antiferromagnetic and half-metallic spin-polarization of edge states in model graphene nanoribbons ( $n$ -acenes) implies a spin contamination  $\langle S^2 \rangle$  that increases proportionally to the length of the ribbon, and diverges to an infinite value in the macroscopic limit. This conclusion is rather worrying, considering that symmetry-broken UDFT approaches are often used to simulate static correlation in extended periodic systems, which cannot be handled with multi-configurational theories. Indeed, a diverging  $\langle S^2 \rangle$  value implies obviously a complete loss of control upon spin- and related electric or magnetic properties in the macroscopic limit of an extended zig-zag graphene nanoribbon (ZGNR).

**Table 1** Evolution of the energy differences of anthracene between “closed shell” RHF/STO-3G and “open-shell” UHF/STO-3G solution as a function of the external electric field. Energy differences are in kcal mol<sup>-1</sup> and electric fields in a.u. (1 a.u.=5.142 10<sup>11</sup> V m<sup>-1</sup>)

Level Electric field	HF $\Delta E(U-R)$	MP2 $\Delta E(U-R)$	MP3 $\Delta E(U-R)$	MP4SDQ $\Delta E(U-R)$	CCSD $\Delta E(U-R)$	CCSD(T) $\Delta E(U-R)$
0.00	-51.43	74.42	68.66	56.22	15.76	15.02
0.01	-50.78	74.35	68.51	56.07	15.63	14.91
0.02	-48.83	74.15	68.03	55.61	15.26	14.57
0.03	-45.58	73.77	67.22	54.82	14.63	13.97
0.04	-41.06	73.12	66.01	53.65	13.73	13.09
0.05	-35.29	72.05	64.31	52.02	12.56	11.88
0.06	-28.39	70.25	61.91	49.74	11.10	10.30
0.07	-20.53	67.11	58.30	46.41	9.31	8.32
0.08	-12.10	61.17	52.25	41.03	7.19	6.03
0.09	-3.98	47.96	39.83	30.49	4.59	3.58
0.10	-0.23	10.21	8.28	5.92	0.71	0.40
0.11	-0.04	3.65	2.92	1.85	0.14	0.07
0.12	-0.53	11.93	9.94	6.57	0.42	0.16
0.13	-1.30	17.53	14.94	10.26	0.59	0.22
0.14	-2.06	21.04	18.20	12.92	0.71	0.27
0.15	-2.67	23.09	20.15	14.73	0.78	0.31
0.16	-3.06	24.03	21.06	15.82	0.83	0.36
0.17	-3.22	24.10	21.13	16.26	0.86	0.41
0.18	-3.23	24.03	20.82	16.24	0.83	0.48
0.19	-3.44	25.05	21.50	17.08	0.98	0.65
0.20	-3.44	26.01	22.12	17.79	1.13	0.81
0.21	-3.26	26.93	22.69	18.36	1.24	0.96
0.22	-2.94	27.62	23.08	18.69	1.32	1.07
0.23	-2.55	27.77	23.03	18.57	1.33	1.14
0.24	0.00	0.00	0.00	0.00	0.00	0.00
0.25	0.00	0.00	0.00	0.00	0.00	0.00

The proof is general and valid for any approximate spin-unrestricted one-determinantal (i.e. HF or DFT) treatment of

**Table 2** The energy differences in-between UB2PLYPD/6-31G results and RB2PLYPD/6-31G results obtained upon RB3LYP/cc-pVTZ geometry. All results are displayed in kcal mol<sup>-1</sup>

n-acenes	$\Delta(U-R)$		
	$\Delta(SCF)$	$\Delta E_2$	$\Delta(B2PLYPD)$
benzene ( $n=1$ )	0.00	0.00	0.00
naphthalene ( $n=2$ )	0.00	0.00	0.00
anthracene ( $n=3$ )	0.00	0.00	0.00
tetracene ( $n=4$ )	-1.40	9.02	7.62
pentacene ( $n=5$ )	-5.22	16.97	11.75
hexacene ( $n=6$ )	-10.29	23.90	13.62
heptacene ( $n=7$ )	-15.85	30.43	14.57
octacene ( $n=8$ )	-21.88	37.04	15.17
nonacene ( $n=9$ )	-28.10	43.73	15.63
decacene ( $n=10$ )	-34.44	50.49	16.05
undecacene ( $n=11$ )	-40.65	57.21	16.56

electron correlation. It employs the formalism of crystalline orbitals for extended systems with periodicity in one dimension, and has the mathematical robustness of a theorem that may be regarded as the counterpart for the  $S^2$  operator of Lieb’s theorem for the total spin momentum,  $S$ . Since graphene nanoribbons and nanoislands have compensated bipartite lattices,  $S$  must be identically zero. In the absence of a spin-dependent potential or perturbation, i.e. in a non-relativistic quantum mechanical framework, the singlet nature of the electronic ground state therefore most clearly rules out any symmetry-breaking, even an infinitesimal one, of spin-densities in an extended zig graphene nanoribbon. Whatever the size of the system, in field-free non relativistic quantum mechanics, symmetry-breakings of spin-densities are necessarily the outcome of a too approximate treatment of electron correlation. A most inconvenient finding in support to this statement is that, at the UHF level, any conjugated compound (including benzene, naphthalene, anthracene, 1,3-butadiene, biphenyl, ...) is subject to singlet instabilities and artefactual stabilizations of the electronic ground state wave function into a symmetry-broken singlet



open-shell state. Symmetry-breakings in spin-densities and spin contamination in spin-unrestricted calculations can also occur in systems with no symmetry point group, but are in this case more difficult to detect. In any case, the most basic principles of symmetry point group theory should never be violated for *singlet* states, even in the context of Density Functional Theory [125].

The probability to observe symmetry breakings varies inversely to the band gap between occupied (valence) and unoccupied (conduction) one-electron states, because of the non-analytic (i.e. iterative) nature of solutions obtained with any self-consistent field (HF, DFT, mean field Hubbard or even CASSCF) procedure. For extended ZGNRs with a vanishingly small band gap, one may argue [21] that, because of the extreme electronic polarizabilities of these systems, sizeable physical symmetry breakings in spin-densities can be induced by marginally small spin-dependent perturbations, typically spin-orbit coupling interactions, of the order of 24  $\mu\text{eV}$  [64]. However, GW band structure calculations on ZGNRs with a width ranging from 0.4 to 2.4 nm indicate band gaps in the range of 0.5–3.0 eV [126], whereas recent quantum chemical calculations on model nanoribbons employing second-order perturbation theory demonstrate that the extent of spin-orbit coupling interactions decreases with increasing system size [127]. In the current state of knowledge, the chances to observe anti-ferromagnetism and half-metallicity in pristine graphene systems seem therefore all in all quite limited.

If half-metallicity is ever demonstrated experimentally for extended zig-zag graphene nanoribbons, one must note that, at this stage, there exist no consistent and accurate enough treatments of physical symmetry breakings of spin-densities due to spin-orbit coupling interactions in these systems. Such treatments would require a characterization of spin-flip and spin disentanglement processes with an accuracy of a few tenths  $\mu\text{eV}$ , which at present clearly goes much beyond all thinkable possibilities in terms of computational facilities and available softwares. We note that, to our knowledge, no direct experimental proof of edge magnetism in pristine graphene has ever been reported so far. Besides, magnetism in graphene is most commonly ascribed to structural defects or impurities [128].

To summarize, we believe that our analysis using crystalline orbitals and our model calculations are altogether robust (and provocative) enough for calling into question the idea that graphene nanoislands and nanoribbons of finite width (including *n*-acenes) are anti-ferromagnetic and half-metallic systems, in the absence of complications such as thermally induced spin-flip processes, structural defects (vacancies, adatoms), or magnetic perturbations, since these views imply sharp contradictions with the implications of Lieb's theorem for compensated bipartite lattices, but also with most basic principles and general theorems of (non-

relativistic) quantum mechanics (antisymmetry principle, group theory, spin quantization). Indeed, at the confines of non-relativistic quantum mechanics, whatever the dimensions of the system of interest, an exact treatment of electron correlation must necessarily repair symmetry breakings into singlet open-shell states, i.e. restore the correct symmetries in spin-up and spin-down densities.

**Acknowledgments** Most calculations presented in this work have been performed on a Compaq ES47 work station at Hasselt University, Belgium. For this work we also used the infrastructure of the VSC Flemish Supercomputer Center, funded by the Hercules foundation and the Flemish Government department EWI. This work has been supported by the FWO-Vlaanderen, the Flemish branch of the Belgian National Science Foundation, and by the BijzonderOnderzoeksFonds (BOF: special research fund) at Hasselt University. M. S. D and B. H. especially acknowledge financial support from a Research Program of the Research Foundation - Flanders (FWO\_Vlaanderen; project number G.0350.09 N, entitled “From orbital imaging to quantum similarity in momentum space”).

## References

1. Novoselov KS, Geim AK, Morozov SV, Jiang D, Zhang Y, Dubonos SV, Grigorieva IV, Firsov AA (2004) *Science* 306:666–669
2. Berger C, Song Z, Li X, Wu X, Brown N, Naud C, Mayou D, Li T, Hass J, Marchenkov AN, Conrad EH, First PN, de Heer WA (2006) *Science* 312:1191–1196
3. Zhang Y, Tan Y-W, Stormer HL, Kim P (2005) *Nature (London)* 438:201–204
4. Novoselov KS, Jiang Z, Zhang Y, Morozov SV, Stormer HL, Zeitler U, Maan JC, Boebinger GS, Kim P, Geim AK (2007) *Science* 315:1379–1379
5. Novoselov KS, Geim AK, Morozov SV, Jiang D, Katsnelson MI, Grigorieva IV, Dubonos SV, Firsov AA (2005) *Nature* 438:197–200
6. Bolotin KI, Ghahari F, Shulman MD, Stormer HL, Kim P (2009) *Nature* 462:196–199
7. Du X, Skachko I, Duerr F, Luican A, Andrei EY (2009) *Nature* 462:192–195
8. Bonaccorso F, Sun Z, Hasan T, Ferrari AC (2010) *Nature Photonics* 4:611–622
9. Han MY, Özyilmaz B, Zhang Y, Kim P (2007) *Phys Rev Lett* 98:206805
10. Williams G, Seger B, Kamat PV (2008) *ACS Nano* 2:1487–1491
11. Fujita M, Wakabayashi K, Nakada K, Kusakabe K (1996) *J Phys Soc Jpn* 65:1920–1923
12. Nakada K, Fujita M, Dresselhaus G, Dresselhaus MS (1996) *Phys Rev B* 54:17954–17961
13. Wakabayashi K, Fujita M, Ajiki H, Sigrist M (1999) *Phys Rev B* 59:8271–8282
14. Miyamoto Y, Nakada K, Fujita M (1999) *Phys Rev B* 59:9858–9861
15. Parr RG, Yang W (1989) *Density functional theory of atoms and molecules*. Oxford University Press, New York
16. Dreizler RM, Gross EKH (1990) *Density functional theory*. Springer-Verlag, Berlin
17. Koch W, Holthausen M (2001) *A chemist's guide to density functional theory*, 2nd. Wiley-VCH, Weinheim
18. Kobayashi Y, Fukui K-I, Enoki T, Kusakabe K, Kaburagi Y (2005) *Phys Rev B* 71:193406

19. Enoki T, Kobayashi Y (2005) *J Mat Chem* 15:3999–4002
20. Niimi Y, Matsui T, Kambara H, Tagami K, Tsukada M, Fukuyama H (2006) *Phys Rev B* 73:085421
21. Son Y-W, Cohen ML, Louie SG (2006) *Nature* 444:347–349
22. Perdew JP, Zunger A (1981) *Phys Rev B* 23:5048–5079
23. Lieb EH (1989) *Phys Rev Lett* 62:1201–1204
24. Okada S, Oshiyama A (2001) *Phys Rev Lett* 87:146803
25. Lee H, Son Y-W, Park N, Han S, Yu J (2005) *Phys Rev B* 72:174431
26. Fernandez-Rossier J, Palacios JJ (2007) *Phys Rev Lett* 99:177204
27. Yazyev OV (2010) *Rep Phys Rep* 73:056501
28. Jiang D, Sumpter BG, Dai S (2007) *J Chem Phys* 127:124703
29. Rudberg E, Salek P, Luo Y (2007) *Nano Lett* 7:2211–2213
30. Silvestrov PG, Efetov KB (2007) *Phys Rev Lett* 98:016802
31. Shemella P, Zhang Y, Mailman M, Ajaya PM, Nayak SK (2007) *Appl Phys Lett* 912:042101
32. Hod O, Barone V, Scuseria GE (2008) *Phys Rev B* 77:035411
33. Hod O, Barone V, Peralta JE, Scuseria GE (2007) *Nano Lett* 7:2295–2299
34. Dutta S, Manna AK, Pati SK (2009) *Phys Rev Lett* 102:096601
35. Dutta S, Pati SK (2010) *Carbon* 48:4409–4413
36. Mañanes A, Duque F, Ayuela A, López MJ, Alonso JA (2008) *Phys Rev B* 78:035432
37. Huang B, Si C, Lee H, Zhao L, Wu JA, Gu BL, Duan WH (2010) *Appl Phys Lett* 97:043115
38. Tang S, Cao Z (2011) *Comput Mater Sci* 50:1917–1924
39. Huang B, Son Z-W, Kim G, Duan W, Ihm J (2009) *J Am Chem Soc* 131:17919–17925
40. Wolf SA, Awschalom DD, Buhrman RA, Daughton JM, von Molnár S, Roukes ML, Chtchelkanova AY, Treger DM (2001) *Science* 294:1488–1495
41. Perdew JP, Burke K, Ernzerhof M (1996) *Phys Rev Lett* 77:3865–3868
42. Perdew JP, Burke K, Ernzerhof M (1997) *Phys Rev Lett* 78:1396–1396
43. Heyd J, Scuseria GE, Ernzerhof M (2003) *J Chem Phys* 118:8207–8215
44. Heyd J, Scuseria GE, Ernzerhof M (2006) *J Chem Phys* 124:219906
45. Izmaylov AF, Scuseria GE, Frisch MJ (2006) *J Chem Phys* 125:104103
46. Bendikov M, Duong HM, Starkey K, Houk KN, Carter EA, Wudl F (2004) *J Am Chem Soc* 126:7416–7417
47. Bendikov M, Duong HM, Starkey K, Houk KN, Carter EA, Wudl F (2004) *J Am Chem Soc* 126:10493–10493
48. Hachmann J, Dorando JJ, Avilés M, Chan GK-L (2007) *J Chem Phys* 127:134309
49. Qu Z, Zhang D, Liu C, Jiang Y (2009) *J Phys Chem A* 113:7909–7914
50. dos Santos MC (2006) *Phys Rev B* 74:045426
51. Jiang D-E, Dai S (2008) *J Phys Chem A* 112:332–335
52. Jiang D-E, Dai S (2008) *Chem Phys Lett* 466:72–75
53. Ishida T, Aihara J (2009) *Phys Chem Chem Phys* 11:7197–7201
54. Jiang D-E, Chen XQ, Luo W, Shelton WA (2009) *Chem Phys Lett* 483:120–123
55. Chen Z, Jiang D-E, Lu X, Bettinger HF, Dai S, Schleyer PvR, Houk KN (2007) *Organic Lett* 9:5449–5452
56. Nesbet RK (1961) *Rev Mod Phys* 33:28–36
57. Löwdin P-O (1963) *Rev Mod Phys* 35:496–501
58. Davidson ER, Borden WT (1983) *J Phys Chem* 87:4783–4790
59. Jensen F (1999) *Introduction to computational chemistry*. Wiley, Chichester
60. Cramer CJ (2004) *Essentials of computational chemistry*, 2nd edn. Wiley & Sons, Chichester
61. Levine IR (1999) *Quantum Chemistry*. 5th ed. Prentice Hall
62. Manne R (1972) *Mol Phys* 24:935
63. Szabo AS, Ostlund NS (1989) *Modern quantum chemistry*. McGraw-Hill, New York
64. Gmitra M, Kunschuh S, Ertl C, Ambrosch-Draxl C, Fabian J (2009) *Phys Rev B* 80:235431
65. André JM, Ladik J (1975) *Electronic structure of polymers and molecular crystals*. Plenum, New York
66. André JM, Delhalle J, Ladik J (1975) *Quantum theory of polymers*. Reidel, New York
67. Ladik J (1980) *Adv Quantum Chem* 12:65
68. Kertesz M (1982) *Adv Quantum Chem* 15:161–214
69. Ladik J, André JM (1984) *Quantum chemistry of polymers: solid state aspects*. Reidel, Dordrecht
70. Ladik J (1988) *Quantum theory of polymers as solids*. Plenum, New York
71. André JM, Delhalle J, Brédas JL (1991) *Quantum chemistry aided design of organic polymers*. World Scientific, London
72. Fripiat JG, Delhalle J, Harris FE (2007) In: Simos TE, Maroulis G (eds) *Computation in Modern Science and Engineering*. American Institute of Physics, Melville, NY, Vol. 2, Pt. A, pp 179–182
73. Born M, Karman T (1912) *Phys Z* 13:297–309
74. Bloch F (1928) *Z Phys* 52:555–600
75. Löwdin PO (1956) *Adv Phys* 5:1
76. Calais JL, Pickup BT, Deleuze MS, Delhalle J (1995) *Eur J Phys* 16:179–186
77. Bube RH (1974) *Electronic properties of crystalline solids—an introduction to fundamentals*. Academic, New York
78. Monkhorst HJ, Kertesz K (1981) *Phys Rev B* 24:3015–3024
79. Delhalle J, Calais JL (1986) *J Chem Phys* 85:5286–5298
80. Deleuze MS, Delhalle J, Pickup BT, Calais J-L (1992) *Phys Rev B* 46:15668–15682
81. Deleuze MS, Delhalle J, Pickup BT, Calais J-L (1995) *Adv Quantum Chem* 26:35–98
82. Deleuze MS, Scheller MK, Cederbaum LS (1995) *J Chem Phys* 103:3578–3588
83. Frisch MJ, Trucks GW, Schlegel HB, Scuseria GE, Robb MA, Cheeseman JR, Scalmani G, Barone V, Mennucci B, Petersson GA, Nakatsuji H, Caricato M, Li X, Hratchian HP, Izmaylov AF, Bloino J, Zheng G, Sonnenberg JL, Hada M, Ehara M, Toyota K, Fukuda R, Hasegawa J, Ishida M, Nakajima T, Honda Y, Kitao O, Nakai H, Vreven T, Montgomery Jr JA, Peralta JE, Ogliaro F, Bearpark, M, Heyd JJ, Brothers E, Kudin KN, Staroverov VN, Kobayashi R, Normand J, Raghavachari K, Rendell A, Burant JC, Iyengar SS, Tomasi J, Cossi M, Rega N, Millam JM, Klene M, Knox JE, Cross JB, Bakken V, Adamo C, Jaramillo J, Gomperts R, Stratmann RE, Yazyev O, Austin AJ, Cammi R, Pomelli C, Ochterski JW, Martin RL, Morokuma K, Zakrzewski VG, Voth GA, Salvador P, Dannenberg JJ, Dapprich S, Daniels AD, Farkas Ö, Foresman JB, Ortiz JV, Cioslowski J, Fox DJ (2009) *Gaussian 09*, Revision A.1. GaussianInc, Wallingford CT
84. Becke AD (1993) *J Chem Phys* 98:1372–1377
85. Lee C, Yang W, Parr RG (1998) *Phys Rev B* 37:785–789
86. Lowe JP, Peterson KA (2005) *Quantum chemistry*. Elsevier, Amsterdam
87. Atkins PW, Friedmann RS (2005) *Molecular Quantum Mechanics*. Oxford University Press
88. Schatz GC, Ratner MA (2002) *Quantum Mechanics in Chemistry*. (Dover Publications, Mineola, New York, or any text book on group theory)
89. Lynch BJ, Fast PL, Harris M, Truhlar DG (2000) *J Phys Chem A* 104:4811–4815
90. Lynch BJ, Truhlar DG (2001) *J Phys Chem A* 105:2936–2941
91. Schwabe T, Grimme S (2007) *Phys Chem Chem Phys* 9:3397–3406
92. Adamo C, Barone V (1998) *J Chem Phys* 108:664–675
93. Jameson CJ, Fowler PW (1986) *J Chem Phys* 85:3432–3436
94. Jasien PG, Fitzgerald G (1990) *J Chem Phys* 93:2554–2560
95. Sim F, Salahub DR (1992) *Int J Quantum Chem* 43:463–479

96. Guan JG, Duffy P, Carter JT, Chong DP, Casida KC, Casida ME, Wrinn M (1993) *J Chem Phys* 98:4753–4765
97. Dixon DA, Matsuzawa N (1994) *J Phys Chem* 98:3967–3977
98. Matsuzawa N, Dixon DA (1994) *J Phys Chem* 98:2545–2554
99. Guan JG, Casida ME, Köster AM, Salahub DR (1995) *Phys Rev B* 52:2184–2200
100. McDowell SAC, Amos RD, Handy NC (1995) *Chem Phys Lett* 235:1–4
101. Matsuzawa N, Ata M, Dixon DA (1995) *J Phys Chem* 99:7698–7706
102. Dunning TH Jr (1989) *J Chem Phys* 90:1007–1023
103. Feller D (1992) *J Chem Phys* 96:6104–6114
104. Feller D (1993) *J Chem Phys* 98:7059–7071
105. Møller C, Plesset MS (1934) *Phys Rev* 46:618–622
106. Krishnan R, Pople JA (1978) *Int J Quantum Chem* 14:91–100
107. Head-Gordon M, Pople JA, Frisch MJ (1988) *Chem Phys Lett* 153:503–506
108. Trucks GW, Watts JD, Salter EA, Bartlett RJ (1988) *Chem Phys Lett* 153:490–495
109. Purvis GD III, Bartlett RJ (1982) *J Chem Phys* 76:1910–1918
110. Raghavachari K, Trucks GW, Pople JA, Head-Gordon M (1989) *Chem Phys Lett* 157:479–483
111. Bartlett RJ, Watts JD, Kucharski SA, Noga J (1990) *Chem Phys Lett* 165:513–522
112. Stanton JF (1997) *Chem Phys Lett* 281:130–134
113. Hajgato B, Huzak M, Deleuze MS (2011) *J Phys Chem A* 115:9282–9293
114. Jaffé HH, Orchin M (1965) *Symmetry in chemistry*. John Wiley & Sons, New York
115. Cederbaum LS, Tarantelli F, Winkler P (1990) *J Phys B* 23:L747–L752
116. Cederbaum LS, Winkler P (1994) *Theor Chim Acta* 88:257–270
117. Huzak M, Deleuze MS, Hajgató B (2011) *J Chem Phys* 135:104704
118. Knight LB Jr, Bell BA, Cobranchi DP, Davidson ER (1999) *J Chem Phys* 111:3145–3154
119. Knight LB Jr, Rice WE, Moore L, Davidson ER, Dailey RS (1998) *J Chem Phys* 109:1409–1424
120. Frisch MJ, Head-Gordon M, Pople JA (1990) *Chem Phys Lett* 166:281–289
121. Pople JA, Binkley JS, Seeger R (1976) *Int J Quantum Chem Suppl* Y-10:1
122. Scuseria GE, Janssen CL, Schaefer HF III (1988) *J Chem Phys* 89:7382–7387
123. Bartlett RJ (1989) *J Phys Chem* 93:1697–1708
124. Grimme S (2006) *J Chem Phys* 124:034108
125. Pople JA, Gill PMW, Handy NC (1995) Spin-contamination is not well-defined in DFT methods. *Int J Quantum Chem* 56:303–305, except if the real interacting function is a spin singlet ( $S=0$ ). For singlet states, therefore, charge- and spin-densities must exhibit the full symmetry of the molecular point group (Perdew JP, Ruzinsky A, Constantin LA, Sin J, Csonka GI (2009) *J Chem Theor Comput* 5:902–908)
126. Yang L, Park CH, Son YW, Cohen ML, Louie SG (2007) *Phys Rev Lett* 99:186801
127. Perumal S, Minaev B, Ågren H (2012) *J Chem Phys* 136:104702
128. Yazyev OV, Helm L (2007) *Phys Rev B* 75:125408